

Impact of SiC colloidal suspension properties for the fabrication of highly porous ceramics

Bijay Basnet^a, Woo Young Jang^a, Jung Gyu Park^a, In Sub Han^b, Tae Young Lim^c, Hyung Mi Lim^c and Ik Jin Kim^{a,*}

^aInstitute of Processing and Application of Inorganic Materials, (PAIM), Department of Advanced Materials Science and Engineering, Hanseo University, 46, Hanseo 1-ro, Haemi-myun, Seosan-si, Chungchungnam-do, 31962, Korea

^bKorea Institute of Energy Research (KIER), #152, Gajeong-gu, Daejeon, 34129, Korea.

^cKorea Institute of Ceramic Engineering & Technology(KICET), Jinju 52851, Korea

This study discusses the impact of colloidal suspension properties on the wet foam stability of porous ceramics obtained by direct foaming from a particle-stabilized colloidal suspension. The influence of binder content on the wet foam stability in terms of rheology, surface tension, average bubble size and air content are reported. The partial hydrophobization of colloidal suspension was carried out by applying Octylamine as surfactant. PEG binder was added as a wet foam stabilizer. The results shows the wet foam stability of more than 90%, which corresponds to an air content of 86.5% with a colloidal suspension containing 20 wt.% of binder. The Newtonian additive, binder decreases viscosity of colloidal suspension to create a favorable condition for wet foam stability. Uniform distribution of highly open/interconnected pores was controlled with an increase in the binder content of up to 20 wt.%, leading to a higher wet foam stability for porous ceramics.

Key words: Colloidal suspension, Rheology, Direct foaming, Wet-foam stability, Porous ceramics.

Introduction

Porous SiC ceramics have attracted a considerable amount of interest due to their special properties such as excellent mechanical strength, good chemical resistance, high thermal conductivity, good thermal shock resistance and excellent filtration properties [1-3]. This makes porous SiC ceramics candidate materials in various industrial applications like, catalytic support, gas and liquid filters, membrane support, light-weight structural parts, grinding materials, etc. The ability to perform the desired function in a particular application depends on the pore morphology of the porous ceramics, so the rheological and colloidal behavior of the suspension strongly that are influenced by the processing route allow control over such characteristics [4, 5].

Surfactant films can reduce the surface tension, which affects the surface viscosity, preventing a collapse in the suspension through an electrostatic force. The pH, rheological effect, and colloidal properties influence the stability of the colloidal suspension [6-8]. The zeta potential expresses the total charging and, accordingly, the correlated electrostatic attraction between the particles. Hence, measuring the zeta potential, i.e. active particle

charging, allows delineating the difference in the surface charge density and system stability. Often, when the zeta potential value is used to evaluate the colloidal suspension, a marginal value of +/-30 mV is considered to be an indication of the physical stability [9-11].

Different processing routes exist for porous ceramics, and direct foaming is particularly suitable to fabricate porous structures with a pore size between 30 mm to 1 mm [12, 13]. Simplicity, environmental friendliness, and a low production cost make direct foaming particularly interesting for industrial manufacturing [14, 15]. Direct foaming involves the production of a porous material through direct incorporation of air into a suspension or liquid media via mechanical frothing, generating air bubbles inside the ceramic suspension. During the processing, the bubbles are incorporated in the wet state that must be set, and in most cases, it must also be sintered either in a gaseous medium or in a vacuum to maintain the pore structure [16, 17].

This study discusses the stability of the colloidal suspension as a function of the zeta potential and rheological properties and colloidal properties with the addition of binder into the colloidal suspension. Particles with a binder stabilize the wet foams, and the wet foams were dried at room temperature and were sintered in argon atmosphere at 2150 °C for an hour to tailor the microstructure of the porous ceramics. The microstructure of the cellular ceramics was characterized via field emission scanning electron microscopy (FESEM), where

*Corresponding author:
Tel : +82-41-660-1441
Fax: +82-41-660-1402
E-mail: ijkim@hanseo.ac.kr

pore morphology, porosity and pore size distribution were analyzed.

Experimental

Material and preparation of suspension

SiC ($d_{50} \sim 0.4 \mu\text{m}$, density 3.17 g/cm^3 , Sintex 15C, Saint Gobain, France) was first dispersed in the de-ionized water by a homogenizer (HM1200D, Lab stirrer, 142K, Korea) for 30 min at the speed of 4000 rpm. Then Octylamine (98% Wako pure chemical industries, Ltd., Japan) was added to the SiC suspension as a surface modifier to hydrophobize the surface of SiC particles. The SiC pre-foam slurry was prepared by addition of Polyethyl glycol (PEG, 200, Sigma-Aldrich, Germany) of different concentration from 5 ~ 20 wt.% of SiC suspension consisting of SiC and Octylamine in de-ionized water. The slurry was mixed by paste mixer for 1 min at 3000 rpm.

The pH of the suspension was adjusted to 10 by adding 4 M NaOH (Yakuri Pure Chemicals, Kyoto, Japan) and/or 10 N HCl (35% Yakuri Pure Chemicals, Japan) drop-wise. Through the addition of the required amount of water, the solid content of the final aqueous suspension was set to 23.8 Vol.%. Binder was added to the final suspension at different wt.% to control the variations of the bubble, pore sizes, and wet foam stability. Rheological properties were examined to get the stable colloidal suspension. After 40-min of stirring, the final suspension was then instantly foamed using mechanical frothing, as shown in Fig. 1.

Zeta potential and rheological properties

Zeta potential measurement was conducted on a zetaprobe (Colloidal Dynamics, North Attleboro, MA, USA) to determine the surface charge and isoelectric point of the SiC colloidal suspension. The suspension was prepared by mixing SiC powder with a density of 3.2 g/ml with DI (deionized) water at a particle concentration of 1.29 wt.%. The zeta potential test was used to determine our required pH value.

The rheological behavior was determined using a rheometer (MCR502, Anton Paar, Germany) with a cone cup (CC 27, cone diameter 27 mm) at temperature $25 \text{ }^\circ\text{C}$ for the SiC slurry and a double gap cup (DG

26.7, cup diameter 26.7 mm) for the PEG binder, which has a relatively low viscosity. The flow curves of the slurries were measured for shear rates from 1/s to 1000/s with variable duration from 10 s to 1 s for 120 s overall.

Colloidal and foam characterization:

The surface tension of the suspension was measured using the pendant drop method (KSV Instruments Ltd, Helsinki, Finland). The colloidal suspension was prepared by adding a different wt.% binder to a suspension containing amphiphile (Octylamine) and the pH was adjusted to 10 by diluting the solution with 10 N HCl to the desired solid content depending on the surface tension. The drop volume was set to a value within the range from 5-10 ml.

The air content was measured by calculating the percentage volume increase of the suspension post-foaming, as follows:

$$\text{Air content} = \frac{(V_{\text{wet foam}} - V_{\text{suspension}}) \times 100}{V_{\text{wet foam}}} \quad (1)$$

where $V_{\text{wet foam}}$ indicates the post-foaming wet-foam volume, and $V_{\text{suspension}}$ indicates the post-foaming suspension volume.

To investigate the wet-foam stability, wet-foam samples were filled into cylindrical molds at a constant volume and were left for 48 h. The foam stability was then evaluated by observing the percentage of the volume loss of the foam as follows:

$$\text{Wet foam stability} = \frac{V_{\text{Final}}}{V_{\text{Initial}}} \times 100 \quad (2)$$

where V_{Final} indicates the wet foam volume after 48 hrs and V_{Initial} indicates the wet foam volume before 48 hrs

After mixing for 40 min, the bubble size and distribution of the colloidal suspension was evaluated using a digital camera, and the linear intercepts were measured via optical microscopy in the transmission mode (Somtech Vision, South Korea).

Drying, sintering, and analysis

The wet foams were filled into cylindrical molds and were left to dry at room temperature ($22 \text{ }^\circ\text{C}$ to $25 \text{ }^\circ\text{C}$) for 24 ~ 48 hrs. After drying at room temperature, the

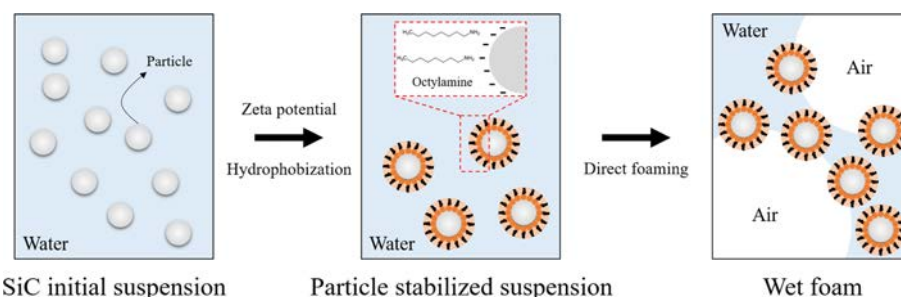


Fig. 1. Schematic diagram of direct-foaming technique to SiC wet foam.

specimens were sintered at 2150 °C for 1 hr in Ar medium. The heating and cooling rates were set to 1 °C/min and 3 °C/min, respectively. The microstructures of the sintered foams were observed using a field-emission scanning electron microscope (FESEM) (JEOL, Japan).

Results and Discussion

Fig. 2 shows the variation in the zeta potential versus the pH of the initial SiC suspension. An initial suspension of 1.29 wt.% was prepared using a micro-sized SiC powder with a density of 3.2 g/ml mixed in de-ionized water. The electrokinetic behavior of the solution was checked via titration with 10 N HCl. The titrant was added dropwise, the zeta potential value sparingly decreased, and the zeta potential value of the suspension exhibited linear behavior from -30 mV to -35 mV when the pH of the solution was made to 9.9 ~ 10.5, which is favorable to produce a stable colloidal suspension [6, 17].

Fig. 3 shows the flow curves of the SiC slurry with different binder content. The viscosity of the SiC slurry decreased as the shear rate increased, exhibiting the typical shear thinning behavior of a non-Newtonian fluid. On the other hand, the individual viscosity of PEG itself is almost constant as the shear rates increases, which is the typical property of a Newtonian fluid. The viscosity of the colloidal suspension decreases with increasing binder content in the colloidal suspension with increase in shear rate. However, the suspension without binder shows higher viscosity for all ranges of shear rates, and this is attributed to the large effect of the Van der Waals forces. Van der Waals forces are always present in a colloidal system [1], and the addition of a binder leads to a considerable decrease in viscosity. The flow curve illustrates that all suspensions exhibit a typical shear-thinning behavior with a decreasing viscosity and increase in shear rate. This shear thinning behavior can be noticed at low shear rates where the

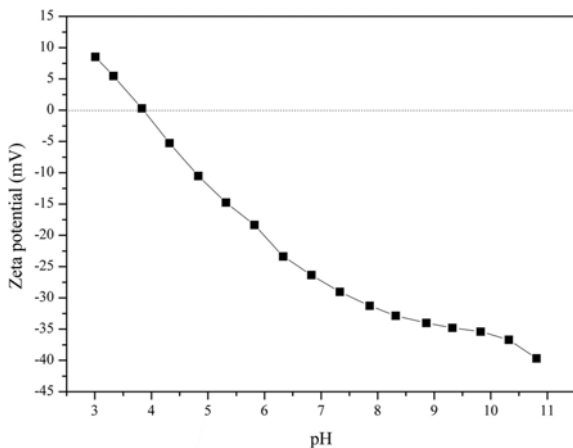


Fig. 2. Zeta potential of the colloidal suspension with respect to pH.

surface forces between particles dominate the rheological behavior [16, 18].

Fig. 4. shows the relation between the surface tension and the average bubble size with respect to the increasing binder content. The result described in the graph shows that the colloidal suspension without a binder exhibits a maximum surface tension of 22.5 mN/m with a larger bubble size of 175 μm . The bubbles contained in the wet foam with a higher surface tension cannot achieve stability as the pressure difference at the air-water interface tends to collapse the bubbles in the wet foam. With an increase in binder content, surface tension of the colloidal suspension decreases with a corresponding decrease in bubble size. The addition of the binder from 15 ~ 20 wt.% results in an optimum surface tension with moderate bubbles sizes of 134 ~ 145 μm with the maximum wet foam stability, as shown in Fig. 7.

Fig. 5 shows the storage and loss modulus analyzed with a varying shear strain, with an amplitude sweep measurement in the oscillation mode. The amplitude sweep of the strain vs modulus, the section for the linear storage modulus (G'), LVE range, and limiting value of the LVE range are selected where the storage modulus begins to decrease. The limiting shear strain

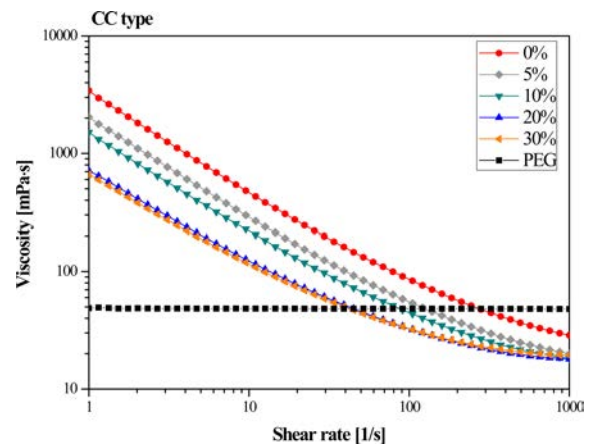


Fig. 3. Effect of the binder content on the viscosity of the colloidal suspension as a function of the shear rate.

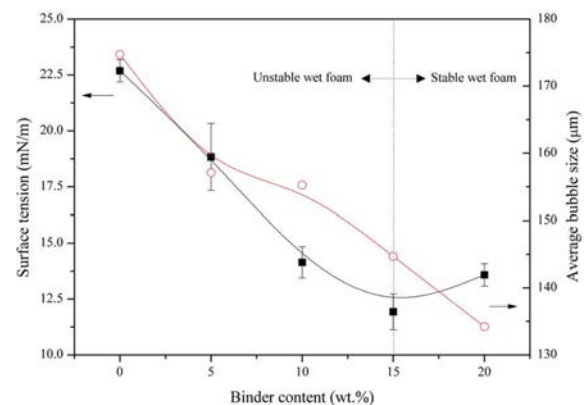


Fig. 4. Surface tension and average bubble with respect to the binder content of the colloidal suspension.

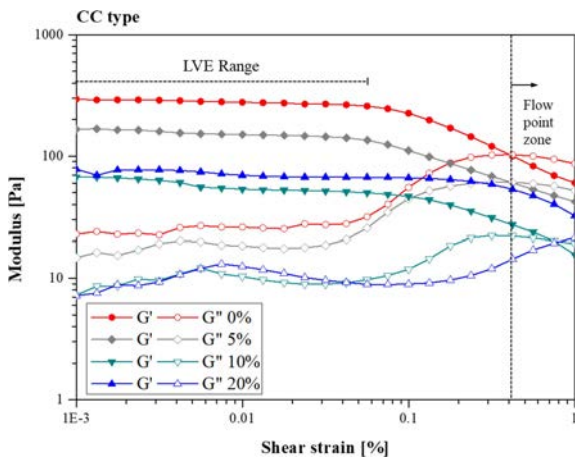


Fig. 5. Oscillation mode amplitude sweep of the slurry with binder contents.

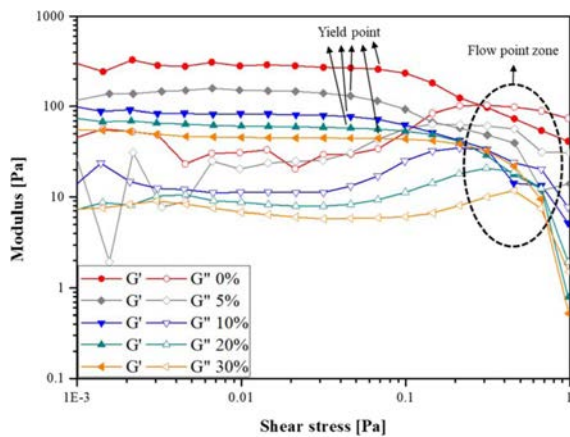


Fig. 6. Oscillation mode amplitude sweep controlled the shear stress of the slurry with binder contents.

of 0.02% was fixed to compare the frequency sweep of the slurries. The storage modulus (G') was measured to be linear and to decrease at the shear strain due to material's internal structure breaks. The storage modulus (G') and the loss modulus (G'') cross where flow begins, which increases as the PEG content increases. The graph shows that the colloidal suspension with more than 10 wt.% binder forms a viscoelastic gel with a high gel strength that shows the strongest resistant to permanent deformation (yielding) under applied stress condition [19]. This composition also shows the highest wet foam stability with air content, as shown in Fig. 9.

Fig. 6 shows the amplitude sweep stress-modulus graph. The value at the limit of the LVE range is called the yield point. At this point, the yield stress is the minimal value of the shear stress applied before the internal structure breaks. The cross point of the storage modulus (G') and loss modulus (G'') is called the flow point, where it finally starts to flow. The G' values of the slurry with PEG content were higher than the G'' values. Over the yield stress, G' and G'' crossed over

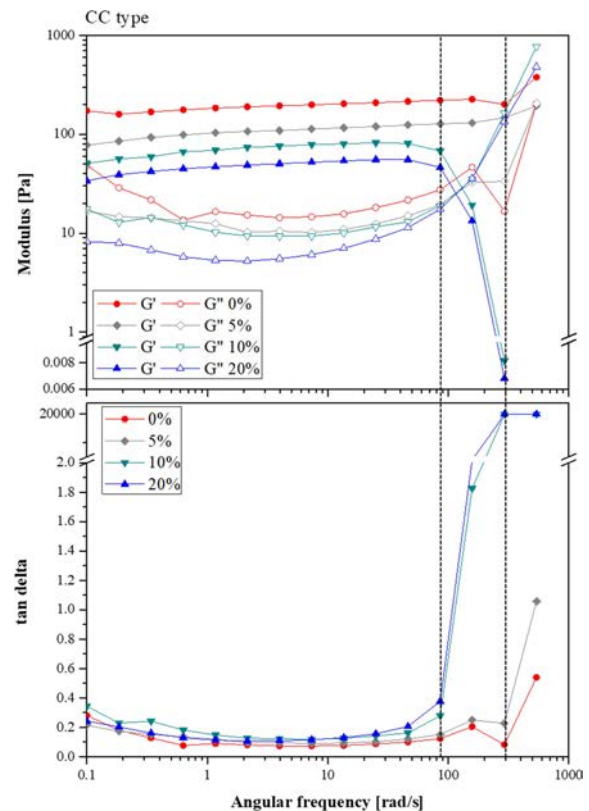


Fig. 7. Oscillation mode frequency sweep of the slurry with binder contents.

so the G' became lower than G'' , and the slurry started to flow. Over the yield stress, the slurry starts to flow, and the particles or the aggregation moved in the slurry. The yield point decreases with an increase in PEG content, and the flow point increases as the PEG content increases except for 0%. The addition of PEG in the slurry made the internal structure break at a smaller shear stress. However, the shear stress of the flow point increases with the addition of PEG content, where the gel-like structure changes to a liquid-like structure. That means the structure is more tightly bound even though the viscosity decreases with the addition of PEG [19].

Fig. 7 shows the frequency sweep, measured by varying the angular frequency at a shear strain of 0.02%. The storage modulus (G') is elastic property of solid, and the loss modulus (G'') is the viscous property of the liquid, $\tan \delta$ is defined as the loss modulus (G'') divided by the storage modulus (G'), where $\tan \delta > 1$ indicates liquid-like behavior and $\tan \delta < 1$ indicates solid-like behavior [20]. The G' values of the slurries were usually higher than the G'' values, and the slurries exhibited a cross over. G' and G'' crossed over so that G' became lower than G'' , and the slurries started to flow after the crossing point. There is an early deviation and vertical elevation of $\tan \delta$ in the colloidal suspension with a higher amount of binder in comparison to the one without binder or less amount of

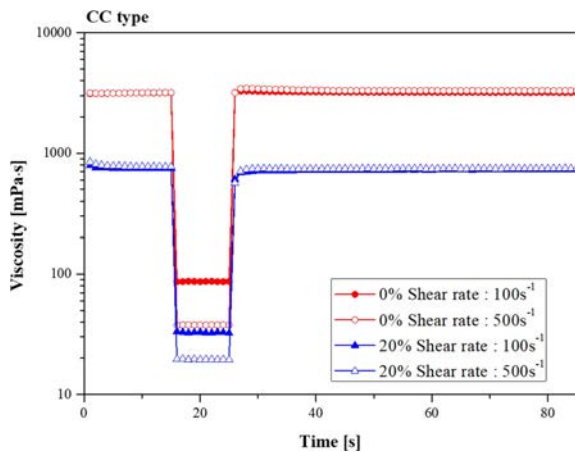


Fig. 8. 3ITT flow curve of 0% and 20% binder contents with different shear rate at different interval.

binder which indicates a favorable condition for the bubble formation. Fig. 7 shows G' and G'' for the SiC slurry with various PEG contents. G'' for the slurry with PEG was higher than G' at a high angular frequency, only where the slurry flowed easily. Most of the slurry behaves as a gel at a frequency of 100 rad/s or lower, and the flow behavior of these slurries was mainly dominated by the particle-particle and particle-PEG attraction and repulsion.

The effect of the time and shear history on the viscosity of the colloidal suspension was studied using 3ITT (Three interval thixotropy test) to understand the structure recovery properties, mostly performed using the controlled shear rate mode, as shown in Fig. 8, with Interval 1 (shear rate 1 s^{-1} , 15 s) - Interval 2 (shear rate 100 s^{-1} or 500 s^{-1} , 10 s) - Interval 3 (shear rate 1 s^{-1} , 60 s). As a typical result, the interval 1 and interval 3 flow curves are presented using linear scales. The analysis for 3 intervals shows when and what percentage of the structure recovery takes place within a certain time period (compared to interval 1). The recovery is faster when the PEG content is not added and at a lower shear rate of Interval 2. The recovery is within 1 sec for the slurry without PEG, the viscosity in Interval 3 increased higher than the viscosity in Interval 1 due to the dispersion at Interval 2 at a high shear rate. The slurry with 20% PEG revealed a higher thixotropy than the slurry without PEG, and recovery is 98% when the shear rate for interval 2 is 100 s^{-1} , and it is 97% when the shear rate of interval 2 is 500 s^{-1} . This higher thixotropy results in a better colloidal suspension for the stable wet foam [19-21].

Fig. 9 shows the relation between the air content and wet foam stability of the SiC suspension, with respect to the added binder content. High volume foams with higher air content were formed upon mechanical frothing, which strongly indicates the stabilization of the wet foam due to the attachment of particles in the air-water interface. The wet foam stability and air

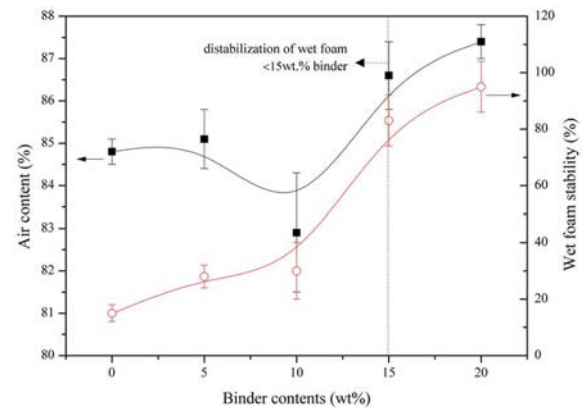


Fig. 9. Air content for wet-foam stability with respect to binder content of colloidal suspension.

content were measured, and an increase in binder content from 5 and 10 wt.% resulted slightly decrease in the air content while the wet foam stability increased. With a further increase in binder content of 15 and 20 wt.%, the air content and wet foam stability sparingly increased to 86.5% and 95% respectively. The addition of the binder content up to 15 wt.% was found less stable where the further addition till 20 wt.% was found to be stable, as shown in Fig. 7 as the destabilization zone. After that, the results show that the wet foam is stable.

In general, the stability of the wet foam of colloidal suspension for porous ceramics was found to be affected by the addition of a binder, and 15 ~ 20 wt.% of binder resulted in the maximum wet foam stability of more than 97%. This study shows that the addition of binder results in shear thinning behavior in a colloidal suspension as shown in Figs. 3, 4 and 5. Also, a decrease in the modulus with respect to the shear strain and angular frequency is seen, and Fig. 5 also shows the effectiveness of the fluid behavior with respect to binder similarly regarding the colloidal properties, as is also seen in Figs. 6, 7 and 8. The condition for the higher wet foam stability was recorded to be best with the binder content of 10 ~ 20 wt.%.

Fig. 10 shows the microstructures of highly porous SiC ceramics sintered for 1 hr at $2150 \text{ }^\circ\text{C}$. Interconnected pores with a pore size ranging up to $350 \text{ }\mu\text{m}$ were obtained. As shown in Fig. 9, the wet foam stability was less than 50% with the 10 wt.% binder content. The dried sample with 10% binder content on sintering resulted in a ceramic body with very weak inter-pore connections, leading to a weak porous ceramic where the sample could be broken simply by applying a force by hand. The microstructure of the sample with 10 wt.% of binder content is shown in Fig. 10(a), clearly shows much less coordination between the pores. The ceramic body with 20 wt.% binder content shows a stronger structure, and the inter-pore connections were also far better than the

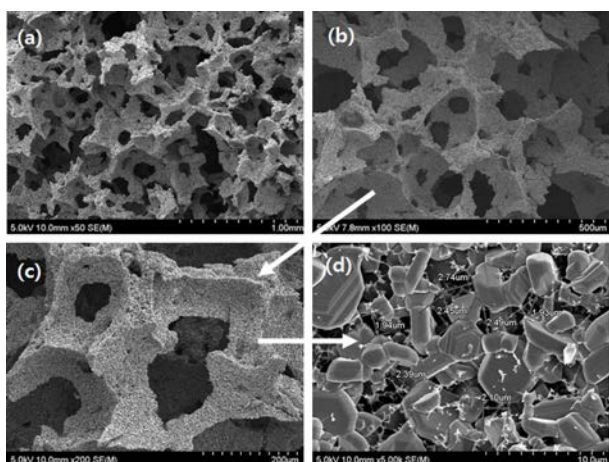


Fig. 10. FESEM image of porous SiC ceramics sintered at 2150 °C for 1 hr with the binder content of (a) 10 wt.% and (b) 20 wt.%, (c) and (d) with different magnification.

sample with 10 wt% of the binder content, as shown in Fig. 10(b) and (c). The sintered body at a higher magnification, as shown in Fig. 10(d) clearly shows high interparticle bonding, which gives the porous ceramic a high mechanical strength. 20 wt.% binder provides good sinter-ability, resulting in ceramics that are applicable for various applications.

Conclusions

The initial SiC colloidal suspension was partially hydrophobized by 12.5 wt.% of Octylamine as a surfactant, and the wet foam was well-stabilized with the use of polyethyl glycol (PEG) binder and after particle stabilization, the mechanical frothing method in direct foaming was used to get the stable wet foams. The results show wet foam stability of more than 85%, with a corresponding air content of more than 80% with an addition of 15 ~ 20 wt.% binder. The addition of binder shows the shear thinning behavior and extends the flow point range. The uniform distribution of the open/interconnected pores could be controlled by increasing the binder content, and this leads to a higher stability of the wet foam with respect to the porous ceramics. The SiC ceramics that are thus produced will be applicable in filters, grinding materials, separation membranes, and many more products to meet global demand.

Acknowledgments

This research was financially supported by Hanseo University and was conducted under the framework of the Research and Development program of the Korea Institute of Energy Research (B6-2455).

References

1. A. Shimamura, M. Fukushima, M. Hotta, T. Ohji and N. Kondo, *J. Ceram. Soc. Japan.* 123[12] (2015) 1106-1108.
2. J.H. Eom, Y.W. Kim, I.H. Song, and H.D. Kim, *J. Eur. Ceram. Soc.* 28 (2008) 1029-1035.
3. M. Fukushima, and P. Colombo, *Sci. Technol. Adv. Mater.* 11 (2010) 16.
4. M. Hotta, H. Kita, H. Matsuura, N. Enomoto, and J. Hojo, *J. Ceram. Soc. Japan.* 120[6] (2012) 243-247.
5. A.R. Studart, U.T. Gonzenbach, E. Tervoort, and L.J. Gauckler, *J. Am. Ceram. Soc.* 89[6] (2006) 1771-1789.
6. J.C.H. Wong, E. Tervoort, S. Busato, U.T. Gonzenbach, A.R. Studart, P. Ermanni, and L.J. Gauckler, *J. Mater. Chem.* 20 (2010) 5628-5640.
7. R. Mouazer, S. Mullens, I. Thijs, J. Luyten, and A. Buekenhoudt, *Adv. Eng. Mat.* 7[12] (2005) 1124-1128.
8. X. Zhang, Y. Zhang, H. Chen, and L. Guo, *J. Adv. Ceram.* 3[2] (2014) 125-131.
9. Z. Yuan, Y. Zhang, Y. Zhou, and S. Dong, *RSC Adv.* 4[92] (2014) 50386-50392.
10. J.S. Lee, S. H. Lee, and S.C. Choi, *All. And Comp.* 467 (2009) 543-549.
11. K. Ohenoja, J. Saari, M. Illikainen, S. B. Faes, A. Kwade, and J. Niinimäki, *Chem. Eng. Technol. Chem. Eng. Technol.* 37[5] (2014) 833-839.
12. F. Li, Z. Kanga, X. Huang, X. G. Wang, and G. J. Zhang, *Chem. Eng. Technol.* 37[5] (2014) 833-839.
13. N. Sarkar, J.G. Park, D.N. Seo, S. Mazumder, A. Pokhrel, C.G. Aneziris, and I.J. Kim, *J. Ceram. Proc. Res.* 16[4] (2015) 392-396.
14. L.Y. Zhang, D.I. Zhou, Y. Chen, B. Liang, and J.B. Zhou, *J. Eur. Ceram. Soc.* 34 (2014) 2443-2452.
15. A. Pokhrel, J.G. Park, W. Zhao, and I.J. Kim, *J. Ceram. Proc. Res.* 13[4] (2012) 420-424.
16. B.S. Murray, *Curr. Opin. Colloid Interface Sci.* 12[4-5] (2007) 232-241.
17. C. Xiaoa, Q. Nib, H. Chen, and L. Guo, *Colloids Surf. A.* 399 (2012) 108-111.
18. R.L. Menchavez, C.R.M. Adavan, and J.M. Calgas, *Mater. Res.* 17[1] (2014) 157-167.
19. A.R. Patel, B. Mankoc, M.D. Bin Sintang, A. Lesaffer, and K. Dewettincka, *RCS. Adv.* 5[13] (2015) 9703-9708.
20. D. Gupta, M. Jassal, and A.K. Agrawal, *RSC Adv.* 6[105] (2016) 102947-102955.
21. I. Butnaru, M.P. Fernández-Ronco, J.C. Polak, M. Heneczowski, M. Bruma, and S. Gaan, *Polym.* 7[8] (2015) 1541-1563.